Density of states for a dielectric superlattice: TE polarization

I. Alvarado-Rodríguez,[1,2,*] P. Halevi,[2] and J. J. Sánchez-Mondragón[1,2]
[1]*Centro de Investigaciones en Ingeniería y Ciencias Aplicadas, Universidad Autónoma del Estado de Morelos, Avenida Universidad 1001, Colonia Chamilpa, Cuernavaca 62210, Mexico*
[2]*Instituto Nacional de Astroísica, Optica y Electrónica, Apartado 51 Puebla, Puebla 72000, Mexico*
(Received 12 August 1998)

We present a calculation of the band structure and the density of states (DOS) for a dielectric one-dimensional superlattice (SL). It is modeled by means of a periodic array of Dirac delta functions, characterized by the grating strength parameter g [Tocci *et al.*, Phys. Rev. A **53**, 2799 (1996)]. The band structure for TE or *s*-polarized modes is given by a simple, compact formula that reproduces well the qualitative features exhibited by a real SL. We make use of equifrequency surfaces in wave-vector space—a concept similar to the electron Fermi surfaces in solid state physics. This is helpful for deriving the DOS as a function of frequency and the g parameter. The slope of the DOS exhibits discontinuities at all the edges of the band gaps. However, the DOS is always finite, unlike the case that wave propagation is restricted to the SL axis (where the DOS vanishes in the band gap). In fact, surprisingly, the DOS is actually *enhanced* relative to free space for all values of the frequency and of g, and especially so at the lower edges of the band gaps. These results are relevant to the spontaneous emission by an atom, or to dipole radiation in one-dimensional periodic structures. [S1063-651X(99)11302-3]

PACS number(s): 42.70.Qs 42.25Bs, 78.20.Bh

I. INTRODUCTION

Sine it was proposed that the emission of electromagnetic radiation can be modified by the environment [1,2], there has been a lot of work in this respect. This work concerns the description of the modification of dipole radiation in several environments like metallic cavities [3,4], dielectric cavities [5], and superlattices (SL's) [6–8]. Such environments are inhomogeneous media, in which either the dielectric constant depends on position or else the medium is homogeneous but bounded, giving rise to boundary conditions. In particular, the periodic dielectric structures have earned a lot of attention because of the possibility of applications on low-threshold microlasers and, more recently, in relation to the advent of information technology [9].

In the case of the SL structures, there are many studies [10,11] on the determination and analysis of the band gaps, the description of the bulk and surface modes, etc. Currently, there is much interest in the band structure of photonic crystals [10], that are two- and three-dimensional generalizations of the superlattice (which may be considered as a special case).

The environmental effects of a periodic dielectric medium have been described by the density of states (DOS) for the electromagnetic field in the medium [12,7]. The DOS is related to the transition rate by means of the Fermi golden rule. Here it is stated that the transition rate is proportional to the interaction dipole field times the DOS at the dipole transition frequency. This is valid to describe the power radiated in one direction.

This paper deals with the calculation of the DOS for the field in a one-dimensional SL. The case of TM polarization is not considered; thus our attention is limited to the TE case. Our model can be viewed as a limiting case of very thin layers with a very large dielectric constant, positioned at equal distances. This is the Dirac δ function model in which these thin layers are represented by a Dirac δ function. It has been used in Ref. [6] in the calculation of the power emission, considering only propagation of light parallel to the SL axis.

The model makes sense if the dielectric constant of the *barriers* is large enough and its thickness is small enough. We derive a simple and compact dispersion relation that gives rise to a band structure which is qualitatively the same as that exhibited by a realistic SL. We have used the concept of *equifrequency surfaces* to aid the calculation of the DOS. Such surfaces arise from the dispersion relation and are the optical equivalent of the *Fermi surfaces* of electrons in solids. The results show an increment of the DOS relative to the free space for all the frequencies and, especially, near the lower band-gap edges. The DOS exhibits discontinuities in the slope at the band edges because of the change in the shape of the equifrequency surface. These results can be extended to a calculation of the power radiated by a dipole in this medium [13].

In Sec. II, we discuss the electromagnetic normal modes for the Dirac δ function model. We derive the corresponding dispersion relation or the band structure and the TE field. We calculate the DOS in Sec. III using the equifrequency surfaces. These surfaces are the optical analogue of the Fermi surfaces for electrons in solids. The conclusions are presented in Sec. IV.

II. NORMAL MODES

A. Dirac δ function model of a superlattice

A Dirac δ function model of a SL is defined by the following dependence of the dielectric constant on the position [6]:

*Present address: Department of Electrical Engineering, University of California at Los Angeles, Los Angeles, CA 90024-7594.

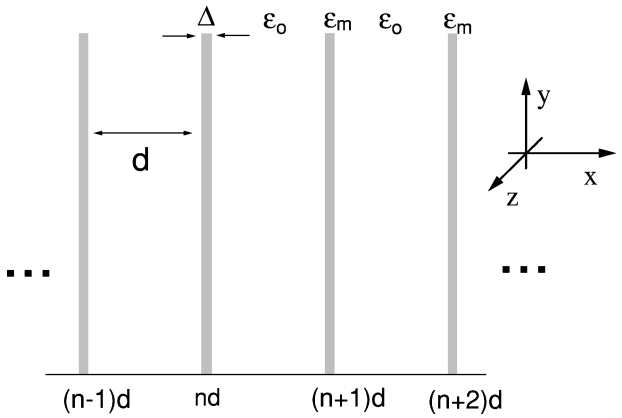

FIG. 1. A Dirac δ superlattice. In this case, $\Delta \to 0$ and $\epsilon_m \to \infty$, while keeping the factor $g=(\epsilon_m-\epsilon_0)\Delta/d$ finite. The stratification direction is the x axis, and the period is denoted by d.

$$\epsilon(x)=\epsilon_0+gd\sum_{n=-\infty}^{\infty}\delta(x-nd). \tag{1}$$

This model can be obtained from Fig. 1 if the widths of the ''barriers'' become vanishingly small ($\Delta \to 0$), and, simultaneously, their dielectric constants increase beyond limit ($\epsilon_m \to \infty$). To understand this approach, compare the integrals $\int_{-d/2}^{d/2}\epsilon(x)dx$ for the model given in Eq. (1) and for the realistic SL consisting of alternating dielectric layers ϵ_o and ϵ_m, whose widths are $d-\Delta$ and Δ, respectively. Then, if g in Eq. (1) is given by

$$g=(\epsilon_m-\epsilon_0)\frac{\Delta}{d}, \tag{2}$$

then the integrals of $\epsilon(x)$, taken for the two models just described, both give $(\epsilon_0+g)d$. Thus taking $\epsilon_m \gg \epsilon_0$ and $\Delta \ll d$ while keeping g constant, we can give a physical meaning to our model Eq. (1). It is expected to become realistic if the dielectric constant ϵ_m is very large and, at the same time, the corresponding layers are very narrow. The g parameter is called the *grating strength.*

This consideration gives some justification to our model, so that its consequences, at least at the qualitative level, will not significantly differ from those that may be obtained from a realistic model. Moreover, the g parameter in Eq. (1) can be adjusted to yield realistic results within a limited frequency range.

B. TE modes

To start with, we have to solve the Maxwell wave equation for an inhomogeneous medium. For a given material geometry, we can describe the field therein as a linear superposition of the normal modes or eigenmodes. Each mode may be labeled according to its wave vector $\mathbf{k}$ and polarization index p. The modes for the electric field are then defined by means of the Helmholtz equation

$$\nabla\times\nabla\times\mathbf{E}_{\mathbf{k}p}(\mathbf{r})-\frac{\omega_{\mathbf{k}p}^2}{c^2}\epsilon(\mathbf{r})\mathbf{E}_{\mathbf{k}p}(\mathbf{r})=\mathbf{0} \tag{3}$$

where the dielectric constant $\epsilon(\mathbf{r})$ is a function of the position due to the inhomogeneity. In this equation, the $\mathbf{E}_{\mathbf{k}p}(\mathbf{r})$ functions represent the monochromatic solutions (eigenvectors) corresponding to the eigenfrequencies $\omega_{\mathbf{k}p}$. To ensure that $\mathbf{E}_{\mathbf{k}p}(\mathbf{r})$ are a complete set of orthonormal functions, they have to fulfill the normalization and closure conditions as stated in Refs. [6,14].

As for any SL, the field can be expressed as a linear combination of the two independent TE and TM polarization modes. Each of these modes satisfies Eq. (3). Here we restrict our calculations of modes and DOS to the TE (s) modes, so that the mode index p, equal to TE, can be suppressed. Because the dielectric constant is independent of y and z, the fields must be proportional to $\exp[i(k_y y+k_z z)]$. For our periodic structure the wave-vector component k_x is given by the Bloch vector k_B which may be restricted to the first Brillouin zone, namely, $-\pi/d<k_B\leqslant\pi/d$. Thus the wave vector is $\mathbf{k}=k_B\hat{\mathbf{x}}+k_y\hat{\mathbf{y}}+k_z\hat{\mathbf{y}}$. Moreover, by the Bloch-Floquet theorem [15,16] the amplitude of the wave is given by a periodic function $u_{\mathbf{k}}(x)$ which has the same period (d) as the given system. Then the electric field is given by

$$\mathbf{E}_{\mathbf{k}}(\mathbf{r})=u_{k_B}(x)e^{ik_B x}e^{i(k_y y+k_z z)}\hat{\mathbf{e}}_{\mathbf{k}} \tag{4}$$

where $\hat{\mathbf{e}}_{\mathbf{k}}$ is a unit vector with arbitrary direction in the yz plane (see Fig. 1), and perpendicular to the wave vector $\mathbf{k}$ as well. Therefore, the polarization vector $\hat{\mathbf{e}}_{\mathbf{k}}$ is

$$\hat{\mathbf{e}}_{\mathbf{k}}=-\frac{k_z}{k_\parallel}\hat{\mathbf{y}}+\frac{k_y}{k_\parallel}\hat{\mathbf{z}}=-\hat{\mathbf{y}}\cos\phi+\hat{\mathbf{z}}\sin\phi \tag{5}$$

where we have defined $k_\parallel$ as the projection of the wave vector on the yz plane, expressed as

$$k_\parallel^2=k_z^2+k_y^2, \tag{6}$$

and ϕ is the angle that $\mathbf{k}$ forms with the z axis. Replacing x by $x+d$ in Eq. (4), we obtain an alternative formulation of the Bloch theorem,

$$\begin{aligned}\mathbf{E}_{\mathbf{k}}(x+d,y,z)&=u(x+d)e^{ik_B x}e^{ik_B d}e^{i(k_y y+k_z z)}\hat{\mathbf{e}}_{\mathbf{k}}\\&=e^{ik_B d}\mathbf{E}_{\mathbf{k}}(x,y,z).\end{aligned} \tag{7}$$

This means that the value of the function one period away from any point is just a phase factor times the value of the function at that point. This phase factor is given by the Bloch wave vector. Substituting Eq. (4) into Eq. (3), we obtain

$$\frac{d^2}{dx^2}\mathbf{E}_{\mathbf{k}}(x)+\left[\frac{\omega_{\mathbf{k}}^2}{c^2}\epsilon(x)-k_y^2-k_z^2\right]\mathbf{E}_{\mathbf{k}}(x)=\mathbf{0}. \tag{8}$$

The solution of this equation, within any two adjacent *barriers* $x=nd$, is the sum of two counterpropagating plane waves in the x direction; this is reasonable as the medium is stratified in this direction. Then

$$\mathbf{E}_{\mathbf{k}}(x)=[Ae^{iKx}+Be^{-iKx}]\hat{\mathbf{e}}_{\mathbf{k}}, \tag{9}$$

where K is given by the dispersion relation in the background medium, which occupies the space between the barriers,

$$K^2=\frac{\omega_{\mathbf{k}}^2}{c^2}\epsilon_0-k_{\parallel}^2. \tag{10}$$

If Eq. (9) represents the solution in the region $n=0$, we can apply the Bloch theorem [Eq. (7)] n times in order to obtain the solution in the nth region,

$$\mathbf{E}_{\mathbf{k}}^{(n)}(x)=e^{ink_Bd}[Ae^{iK(x-nd)}+Be^{-iK(x-nd)}]\hat{\mathbf{e}}_{\mathbf{k}}, \tag{11}$$

where

$$nd<x<(n+1)d. \tag{12}$$

Equation (11) can be rearranged to satisfy Eq. (4).

C. Boundary conditions

Because of the particular model in Eq. (1) that we are considering, the TE boundary conditions have to be formulated in a rather different way than for the usual problem of propagation in a periodic medium [15]. Our derivation is analogous to the scalar-wave calculation of Dowling and Bowden [6]. Faraday's law can be applied, as usual, to any loop centered at a barrier, $x=nd$. Because the magnetic field must be finite, the electric field is continuous across the barriers. Thus the first boundary condition is

$$\mathbf{E}_{\mathbf{k}}^{(n)}(nd)=\mathbf{E}_{\mathbf{k}}^{(n-1)}(nd) \tag{13}$$

The first order derivative, however, is not continuous. To set the boundary condition for the first order derivative, we integrate the Helmholtz equation (8) over a small region near $x=nd$, using Eq. (1), that is

$$\int_{nd-\epsilon}^{nd+\epsilon}dx\,\frac{d^2}{dx^2}\mathbf{E}_{\mathbf{k}}(x)=-K^2\int_{nd-\epsilon}^{nd+\epsilon}dx\,\mathbf{E}_{\mathbf{k}}(x)-\frac{\omega_{\mathbf{k}}^2}{c^2}\int_{nd-\epsilon}^{nd+\epsilon}dx\,gd\sum_n\,\delta(x-nd)\mathbf{E}_{\mathbf{k}}(x). \tag{14}$$

Here the integration interval is small enough so that the function can be taken as a constant which is the function evaluated at $x=nd$. Then the integration results in

$$\frac{d}{dx}\mathbf{E}_{\mathbf{k}}^{(n)}(nd)-\frac{d}{dx}\mathbf{E}_{\mathbf{k}}^{(n-1)}(nd)=-\frac{\omega_{\mathbf{k}}^2}{c^2}gd\mathbf{E}_{\mathbf{k}}(nd), \tag{15}$$

which is the second boundary condition.

D. Solution of the eigenvalue problem; the band structure

Substitution of Eq. (11) into Eqs. (13) and (15) leads to the homogeneous system

$$\mathbf{M}\begin{pmatrix}A\\B\end{pmatrix}=0. \tag{16}$$

The characteristic matrix $\mathbf{M}$ of the system is defined as

$$\mathbf{M}=\begin{pmatrix}1-\exp[i(K-k_B)d] & 1-\exp[-i(K+k_B)d]\\ 1-\exp[i(K-k_B)d]-i\alpha(\omega_{\mathbf{k}},K) & -1+\exp[-i(K+k_B)d]-i\alpha(\omega_{\mathbf{k}},K)\end{pmatrix}, \tag{17}$$

where we have defined $\alpha(\omega_{\mathbf{k}},K)$ as

$$\alpha(\omega_{\mathbf{k}},K)=\frac{gd\omega_{\mathbf{k}}^2}{2c^2K}. \tag{18}$$

To avoid the trivial solution, we have that $\det\mathbf{M}=0$. Then we find the dispersion relation in terms of the Bloch wave vector k_B and $K(\omega_{\mathbf{k}},k_{\parallel})$, as defined in Eq. (10),

$$\cos(k_Bd)=\cos(Kd)-\alpha(\omega_{\mathbf{k}},K)\sin(Kd)\equiv f(K;\omega_{\mathbf{k}}). \tag{19}$$

This equation gives, implicitly, the eigenfrequencies $\omega_{\mathbf{k}}$ as a function of the wave-vector components k_B and $k_{\parallel}$. This dispersion relation was obtained by Dowling and Bowden [6] for the case $k_{\parallel}=0$, namely, with $K=(\omega/c)\sqrt{\epsilon_0}$. K can be either real or purely imaginary, since both types of solutions fulfill the wave equation and the boundary conditions. Now we can see from Eq. (19) that $|f(K;\omega_{\mathbf{k}})|$ can be greater than one for certain ranges of values of K, giving rise to complex solutions for the Bloch wave vector k_B. In these cases, there are band gaps in which, for an (infinite) periodic medium, no solutions exist for the field. We plot this band structure in Fig. 2 for a grating strength $g=0.1$. In this plot, the shadowed areas indicate the allowed regions. From this figure it can be seen that the Dirac δ function model actually reproduces all the qualitative features of a realistic band structure [15]. As the grating strength g increases, the band gaps become wider. Nevertheless, this model has the interesting particularity that the upper edges of all the band gaps are inde-

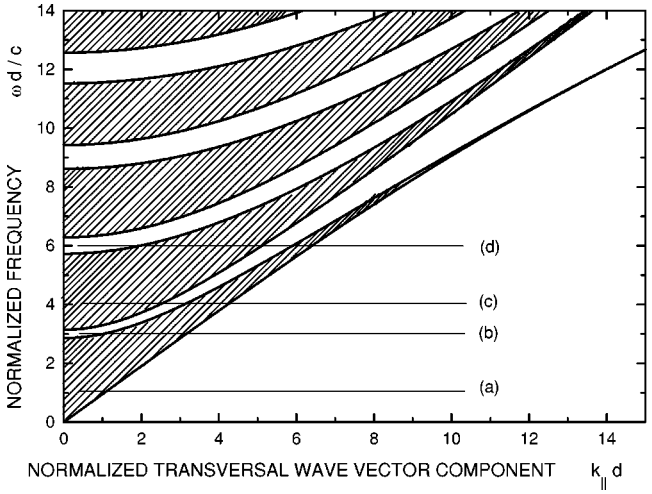

FIG. 2. Band structure for the superlattice in Fig. 1, obtained using the dispersion relation given in Eq. (19) for $\epsilon_0=1$ and $g=0.1$. The width of the forbidden bands increases with g. This means that, with increasing g, the upper band edges are lowered (the lower band edges are ''pinned'' at integer multiples of π for this model). The free-space dispersion relation is recovered in the limit $g\to 0$. This band structure is very similar to that obtained for a realistic superlattice.

pendent of g. In fact, it is easy to show from Eqs. (19) and (10) (with $k_\parallel=0$) that these edges are given by $\omega d/c=n\pi$ $(n=1,2,\ldots)$.

Using Eqs. (16) and (17), we relate the coefficients A and B as

$$B=-\frac{1-e^{i(K-k_B)d}}{1-e^{-i(K+k_B)d}}A, \tag{20}$$

and the total field, from Eqs. (11) and (20), may be expressed as

$$\mathbf{E}_{\mathbf{k}}^{(n)}(x)=\frac{2iAe^{ink_Bd}}{1-e^{-i(K+k_B)d}}(\sin K(x-nd) - e^{-ik_Bd}\sin K[x-(n+1)d])\hat{\mathbf{e}}_{\mathbf{k}}. \tag{21}$$

The constant A is arbitrary.

III. DENSITY OF STATES

We calculate the photon DOS for our SL model for the TE polarization modes. In this case we have to consider that we have continuous electromagnetic bands separated by the band gaps forbidden for propagation.

We study the surfaces of constant frequency (equifrequency surfaces) in **k** space which are constructed with the aid of the dispersion relation, Eq. (19). Similar surfaces for the electron energy eigenvalues are known in solid state physics as *Fermi surfaces* [16], a concept that is also useful for electromagnetic propagation and optical properties. In Fig. 3 several $\omega(k_B,k_y,k_z)=$const curves are sketched in a two-dimensional plot. Due to the azimuthal symmetry of the problem, we can obtain the three-dimensional equifrequency surface $\omega(k_B,k_y,k_z)=$const simply by rotating the curves around the k_B axis.

To describe the surfaces depicted in Fig. 3, take a look at the band structure in Fig. 2. In this figure, horizontal lines are drawn at the frequency values selected in Figs. 3(a), 3(b), 3(c), and 3(d). Line (a) lies entirely within the lowest allowed band, so that the equifrequency surface is closed. Line (b), corresponding to a greater frequency, lies in part in the first band gap and in part in the first band. This produces an interruption in the corresponding equifrequency surface for values $k_\parallel d<1$, as no solutions for the field exist therein. As the frequency keeps increasing, the line $\omega=$const cuts through more and more passbands, so that the equifrequency surfaces split into several sections. This can be seen from Figs. 3(c) and 3(d) with the aid of the corresponding frequency lines transversing the band structure. These surfaces grow in size with the frequency, as we can see from the $k_\parallel$ range for each value of the frequency.

Notice that $k_\parallel$ can exceed the value of $\sqrt{\epsilon_0}\omega/c$. The modes located in the part of the surface where $k_\parallel > \sqrt{\epsilon_0}\omega_{\mathbf{k}}/c$ correspond to the case of imaginary K, and hence to evanescent solutions for $\mathbf{E}_{\mathbf{k}}^{(n)}(x)$, Eq. (21), in the regions between the barriers.

To perform the DOS calculation, it is required to use its formal definition which is the number of available photon modes per unit frequency range. We then construct two equifrequency surfaces, namely, $\omega(k_B,k_y,k_z)=\omega$ and $\omega(k_B,k_y,k_z)=\omega+\Delta\omega$, where ω is an arbitrary value of the frequency and $\Delta\omega$ is a small increment. We calculate the volume therein, and divide it by the volume occupied by a single mode. Then the differential volume element in **k** space within the surfaces is given by (see Fig. 4)

$$\Delta V_k=2\pi k_\parallel \Delta\kappa_t\Delta\kappa_n. \tag{22}$$

Here $\Delta\kappa_t=[(\Delta k_B)^2+(\Delta k_\parallel)^2]^{1/2}$ is a differential segment parallel to the equifrequency surface, and $\Delta\kappa_n$ is the separation of the two surfaces that corresponds to the frequency increment. In order to obtain Eq. (22), it is necessary to rotate the area element $\Delta\kappa_t\Delta\kappa_n$ around the $k_\parallel$ axis. Now $\Delta\kappa_n$ is perpendicular to the surface, and, hence, by definition,

$$\Delta\kappa_n=\frac{\Delta\omega}{|\nabla_{\mathbf{k}}\omega|}. \tag{23}$$

Substituting Eq. (23) into Eq. (22), and integrating over the equifrequency surface, we have that the total phase-space volume contributing to the frequency range $(\omega,\omega+d\omega)$ is

$$\int_{\omega_{\mathbf{k}}} dV_k=2\pi\, d\omega\int_{\omega_{\mathbf{k}}}\frac{k_\parallel}{|\nabla_{\mathbf{k}}\omega|}d\kappa_t, \tag{24}$$

where we take the limit of infinitesimal increments. The number of modes within the range $(\omega,\omega+d\omega)$ is obtained by dividing the volume calculated in Eq. (24) by the volume corresponding to one mode, $(2\pi)^3/V$, where V is the volume of the system. This yields

$$dN(\omega)=\frac{V}{4\pi^2}\left[\int_{\omega_{\mathbf{k}}}\frac{k_\parallel}{|\nabla_{\mathbf{k}}\omega|}d\kappa_t\right]d\omega\equiv D(\omega)d\omega. \tag{25}$$

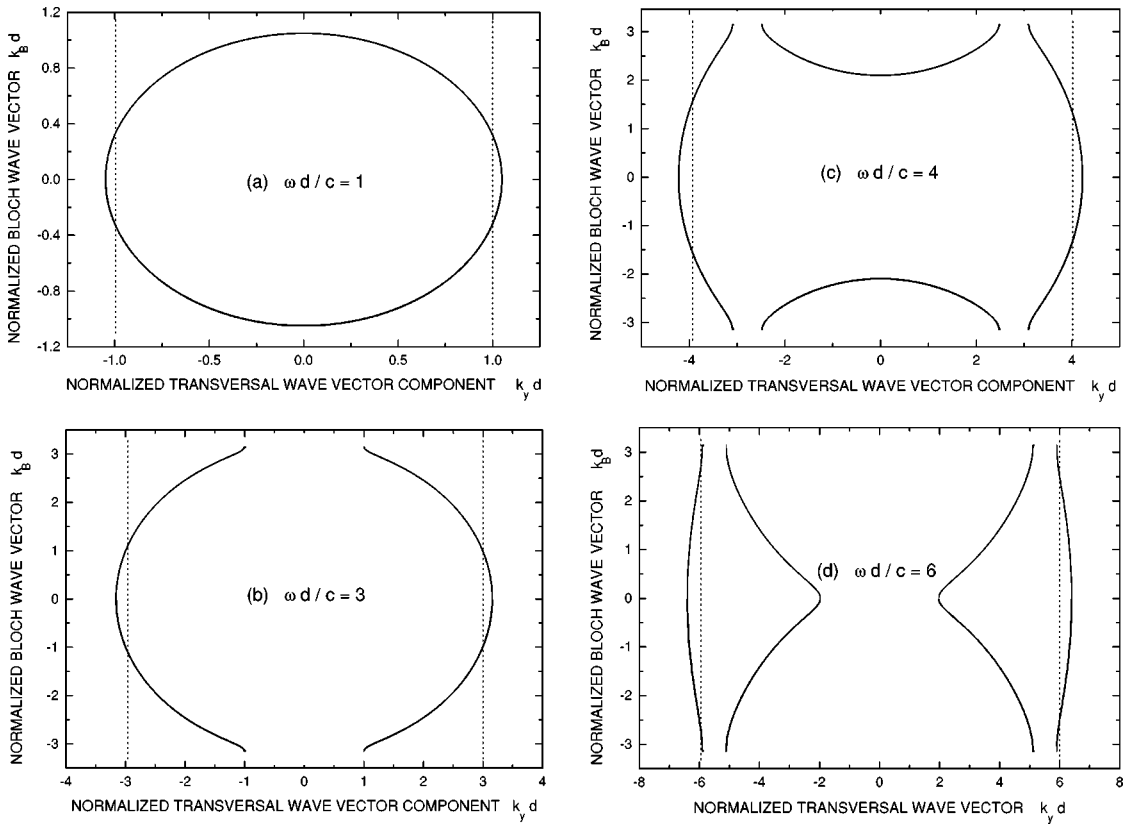

FIG. 3. Four cross sections ($k_z=0$) of equifrequency surfaces $\omega(k_B,k_y,k_z)=\omega=\text{const}$ for $g=0.1$. Due to the azimutal symmetry, the surfaces are formed by rotating the curves around the k_B axis. The dashed lines denote $|k_y|=\omega/c$, so that the region between (outside) these lines is characterized by real (imaginary) K values. (a) Equifrequency surface for $\omega d/c=1$. (b) $\omega d/c=3$; the region $k_\parallel d<1$ is excluded from the surface because such values of $k_\parallel d$ lie in the forbidden band (see Fig. 2). (c) $\omega d/c=4$. (d) $\omega d/c=6$; notice the further splitting of the surfaces due to the apparition of more forbidden bands (the regions $k_\parallel d<2$ and $5<k_\parallel d<6$ are now excluded).

Because ω is a function of $\mathbf{k}$, we can write

$$\nabla_{\mathbf{k}}\omega=\frac{\partial\omega}{\partial k_B}\hat{\mathbf{x}}+\frac{\partial\omega}{\partial k_y}\hat{\mathbf{y}}+\frac{\partial\omega}{\partial k_z}\hat{\mathbf{z}}. \tag{26}$$

By the use of Eqs. (19), (10), and (6) we have that

$$|\nabla_{\mathbf{k}}\omega|=\frac{c^2}{\omega_k}\left|\frac{K\sin k_B d}{(g+\epsilon_0)\sin Kd+(g\omega^2 d/2c^2K)\,\epsilon_0[\cos Kd-(1/Kd)\sin Kd]}\hat{\mathbf{x}}+\frac{k_y}{\epsilon_0}\hat{\mathbf{y}}+\frac{k_z}{\epsilon_{0\text{-}}}\hat{\mathbf{z}}\right|. \tag{27}$$

Then, the final expression for the DOS is

$$D(\omega)=\frac{V\epsilon_0\omega}{4\pi^2c^2}\int_{\omega_k}d\kappa_t\frac{k_\parallel F(\omega,K(\omega,k_\parallel))}{\{K^2[\sin^2 Kd+\alpha(\omega,K)\sin 2Kd-\alpha^2(\omega,K)\sin^2 Kd]+k_\parallel^2F(\omega,K(\omega,k_\parallel))\}^{1/2}}, \tag{28}$$

where we have defined the function $F(\omega,K(\omega,k_\parallel))$ as

$$F(\omega,K(\omega,k_\parallel))\equiv(g/\epsilon_0+1)\sin Kd+\alpha(\omega,K)\times\left[\cos Kd-\frac{1}{Kd}\sin Kd\right]. \tag{29}$$

For frequencies above the first band, the gaps in the equifrequency surfaces must be carefully avoided [see Figs. 3(b)–3(d)] when performing the integration. It is important to note that, even though the group velocity $|\nabla_{\mathbf{k}}\omega|$ vanishes for on-axis propagation ($k_\parallel=0$), at the band edges the density of states remains finite. For other values of $k_\parallel$ always $|\nabla_{\mathbf{k}}\omega|\neq 0$. Nevertheless for frequencies at the band edges, care should be taken when performing a calculation. Indeed, we took the limits of frequencies approaching these edges, this process giving rise to convergence.

We plot the DOS [Eq. (28)] for different values of g in Fig. 5. The inset in this figure shows a plot for a larger range of frequencies. It is seen that there are sharp discontinuities

in the first order derivative at certain values of the frequency. These discontinuities arise from the band gaps of the band structure. For $g=0.1$ the band structure is given in Fig. 2. This value of $g(\ll 1)$ corresponds to a weak modulation of the dielectric constant, so that the $D(\omega)$ curve lies quite close to the free-space DOS (dashed). Nevertheless, the slope $dD(\omega)/d\omega$ suffers an abrupt decrease for $d\omega/c=2.858$, and then an increase for $d\omega/c=\pi$. These values of the frequency are, precisely, the lower and upper edges of the first band gap for $k_{\|}=0$; see Fig. 2. A similar decrease and subsequent increase of the slope reoccurs for the normalized frequencies 5.75 and 2π (see the inset). These values are just the bounds of the second band gap. Of course, because we have allowed for propagation in an arbitrary direction—not merely along the axis of the SL—there are allowed modes for every value of ω, so that the DOS never vanishes.

For increasing values of the grating strength g the $D(\omega)$ curves move further away from the free-space curve. In addition, the discontinuities become longer, simply because the gaps increase with g. The most eyecatching effect is that sharp peaks appear at the lower edges of the gaps, and are, however, resolved only for substantial values of g. This is to say that, not surprisingly, the DOS decreases every time that ω crosses the threshold between a band and a gap. Also notice that the increase in the slope occurs at $d\omega/c=\pi$ for all g. This is because the upper edges of the band gaps are independent of g for our Dirac δ function model, as noted above.

In Fig. 5 an increment of the DOS relative to free space is present for all frequencies, and is particularly pronounced for frequencies near the lower edges of the band gaps. The enhancement increases rapidly with the grating strength parameter g. This can be understood qualitatively from the fact that the DOS of an inlimited, homogeneous dielectric is $(\omega^2/2\pi^2c^3)\epsilon^{3/2}$ per unit volume. For our model [Eq. (1)], the average dielectric constant of the superlattice is $\langle\epsilon(x)\rangle=\epsilon_0+g$. Therefore, ignoring the structure of the superlattice, one could expect an enhancement of the DOS that is proportional to $(\epsilon_0+g)^{3/2}$. For $g=0.9$, this is an enhancement by a factor of about 2.6 with respect to vacuum. However, no need to say, the structure does matter greatly, as manifest especially at the band edges. Thus, a reduction of the DOS with respect to free space does not occur; this despite the fact that, *for one-dimensional propagation*, the DOS actually vanishes for frequencies within the one-dimensional gaps.

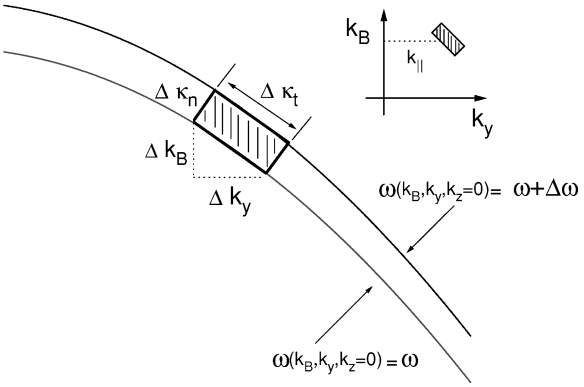

FIG. 4. Partial cross sections in the $k_z=0$ plane of two equifrequency surfaces denoted by ω and $\omega+\Delta\omega$. It is seen that $(\Delta\kappa_t)^2=(\Delta k_B)^2+(\Delta k_{\|})^2$. Using the azimutal symmetry, the total volume element is $\Delta V_k=2\pi k_{\|}\Delta\kappa_t\Delta\kappa_n$, and has the shape of a ring of a rectangular cross section.

IV. CONCLUSION

We have presented a calculation of the modes and of the density of states for a periodic dielectric medium. The calculation is restricted to the TE polarization mode. We made use of a Dirac δ function model, characterized by the grating strength parameter g, as an approximation to the real SL.

A solution of the inhomogeneous wave equation was presented with the aid of the Bloch theorem. A very simple, compact formula was derived for the dispersion relation, and the resulting band structure is found to be qualitatively simi-

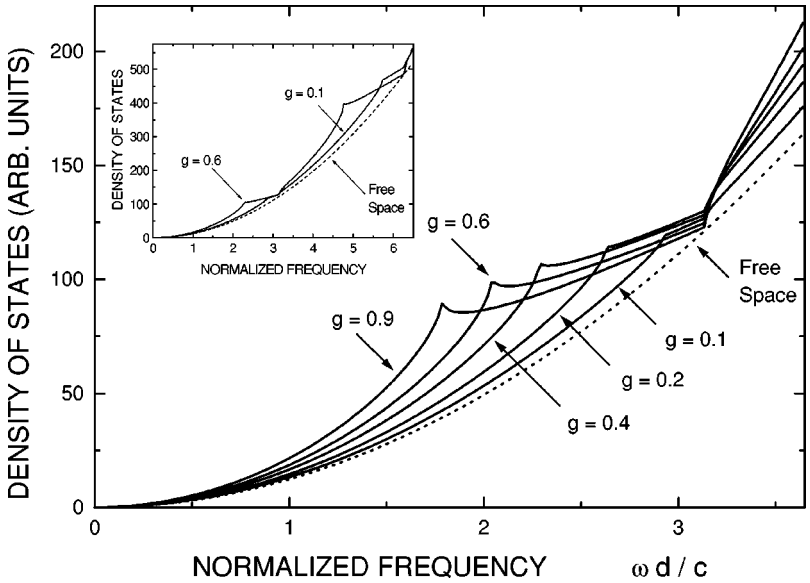

FIG. 5. Density of states as a function of the reduced frequency $\omega d/c$ for several values of the grating strength g. The inset extends the frequency range to the interval $(0,2\pi)$. Here we can see the discontinuities in the slope for frequencies that define the band edges. Notice that the DOS is enhanced for all the values of ω and g, and especially at the lower edges of the band gaps.

lar to that obtained for a realistic SL. Hence, the Dirac δ function model is expected to give reasonable results for the DOS.

The DOS was calculated with the aid of the equifrequency surfaces which are similar to the Fermi surfaces for electrons in solids. Within any one band the DOS increases monotonously with the frequency, reaching a sharp and narrow maximum at the upper band edge (for $k_{\|}=0$). Also, upon crossing from a stop band into a pass band (again for $k_{\|}=0$) there is an abrupt increase in the DOS. The results exhibit an enhancement of the DOS, in comparison to free space, for all values of the frequency. This enhancement increases with the grating strength g [as can be expected from the fact that $\langle \epsilon(x) \rangle$ is proportional to $(\epsilon_0+g)^{3/2}$)], and is especially pronounced at the lower band edges of the band gaps. This behavior is the result of our taking into account propagation in all directions in space. As a consequence, the DOS never vanishes, as occurs if the wave is restricted to propagate along the axis of the SL [6]. Nevertheless, intuitively, one would have expected at least some reduction of the DOS associated with the partial gaps. The fact that this can never happen is rather surprising. These conclusions should be helpful for understanding spontaneous emission (or dipole radiation) in laminated structures. A similar analysis of the DOS for the TM polarization mode is clearly desirable, and will be undertaken in the future.

ACKNOWLEDGMENTS

I.A.R. thanks the CONACyT and SNI for financial support.

[1] E. M. Purcell, Phys. Rev. **69**, 618 (1946).
[2] D. Kleppner, Phys. Rev. Lett. **47**, 233 (1981).
[3] P. W. Milloni and P. L. Knight, Opt. Commun. **9**, 119 (1973); A. O. Barut and J. P. Dowling, Phys. Rev. A **36**, 649 (1987); I. Abram and G. Bourdon, *ibid.* **54**, 3476 (1996); F. de Martini, M. Marrocco, P. Mataloni, L. Crescentini, and R. Loudon, *ibid.* **43**, 2480 (1991); M. A. Rippin and P. L. Knight, J. Mod. Opt. **43**, 807 (1996).
[4] I. Alvardo-Rodríguez, P. Halevi, and J. J. Sańchez-Mondragón, Rev. Mex. Fis. **44**, 268 (1998).
[5] Y. Yamamoto, S. Machida, Y. Horikoshi, and K. Igeta, Opt. Commun. **50**, 337 (1991); R. J. Ram and D. I. Babic, IEEE J. Quantum Electron. **31**, 2 (1995); H. Rigneault and S. Monneret, Phys. Rev. A **54**, 2356 (1996); S. Ciancaleoni, P. Mataloni, O. Jedrkiewicz, and F. De Martini, J. Opt. Soc. Am. B **14**, 1556 (1997).
[6] J. P. Dowling and C. M. Bowden, Phys. Rev. A **46**, 612 (1992).
[7] Toshio Suzuki and Paul K. L. Yu, J. Opt. Soc. Am. B **12**, 570 (1995).
[8] A. Kamli, M. Babiker, A. Al-Hairy, and N. Enfati, Phys. Rev. A **55**, 1454 (1997).
[9] J. D. Joannopoulos, Pierre R. Villenueve, and Shanhui Fan, Nature (London) **386**, 143 (1997).
[10] J. D. Joannopoulos, R. D. Meade, and J. J. Winn, *Photonic Crystals: Molding the Flow of Light* (Princeton University Press, Princeton, 1995).
[11] F. Ramos-Mendieta and P. Halevi, Opt. Commun. **129**, 1 (1996); J. Opt. Soc. Am. B **14**, 370 (1997), and references therein.
[12] Michael D. Tocci, Michael Scalora, Mark J. Bloemer, J. P. Dowling, and C. M. Bowden, Phys. Rev. A **53**, 2799 (1996).
[13] I. Alvarado-Rodríguez and P. Halevi (unpublished).
[14] R. J. Glauber and M. Lewenstein, Phys. Rev. A **43**, 467 (1991).
[15] P. Yeh, *Optical Waves in Layered Media* (Wiley, New York, 1988).
[16] C. Kittel, *Introduction to Solid State Physics* (Wiley, New York, 1976).